Ancient TL

IRSL dating of fast-fading sanidine feldspars from Sulawesi, Indonesia

Bo Li[1*], Richard G. Roberts[1], Adam Brumm[2,3],
Yu-Jie Guo[1], Budianto Hakim[4], Muhammad Ramli[5], Maxime Aubert[6,2],
Rainer Grün[2], Jian-xin Zhao[7], E. Wahyu Saptomo[8,1]

[1] Centre for Archaeological Science, School of Earth and Environmental Sciences
University of Wollongong, New South Wales, Australia
[2]Research Centre of Human Evolution, Environmental Futures Research Institute,
Griffith University, Queensland, Australia
[3] School of Earth and Environmental Sciences, University of Wollongong, New South Wales, Australia
[4] Balai Arkeologi Makassar, Indonesia
[5] Balai Pelestarian Cagar Budaya, Jambi, Indonesia
[6] Place, Evolution and Rock Art Heritage Unit (PERAHU), Griffith University, Queensland, Australia
[7] School of Earth Sciences, University of Queensland, Brisbane, Queensland, Australia
[8] Pusat Penelitian Arkeologi Nasional, Jakarta, Indonesia

*Corresponding Author: bli@uow.edu.au
Received: August 10, 2016; in final form: August 31, 2016

Abstract

The volcanic origin of the sediments from Sulawesi, Indonesia, provides a particular challenge for luminescence dating due to the dim optically stimulated luminescence (OSL) from quartz, and the high anomalous fading rate in the infrared (IR) stimulated luminescence (IRSL) from feldspars. In this study, we present results of dating the sanidine feldspars from 2 samples taken from an archaeological site (Leang Bulu Bettue) in the Maros karsts of South Sulawesi. We tested the post-IR IRSL (pIRIR) procedures in order to find a stable luminescence signal that is less affected by anomalous fading. It was found that there is a highly variable anomalous fading rate in the IRSL and pIRIR signals for different grains and aliquots, and a low temperature IR stimulation (at 50 °C or 100 °C) used in a pIRIR procedure cannot completely remove the anomalous fading for the subsequent pIRIR signals. The large uncertainties associated with fading rates prevent the application of fading-correction procedures. We propose a method to obtain reliable D_e estimates by extrapolation of the relationship between D_e and laboratory fading rate (g-value). The resultant luminescence ages show consistency with other radiometric age determinations from the site. Our results suggest that a systematic and detailed investigation of the relationship between D_e and anomalous fading rate for different grains or aliquots is necessary for dating volcanic feldspars.

Keywords: Post-IR IRSL, Volcanic feldspars, Sanidine, Luminescence dating, Sulawesi, Indonesia

1. Introduction

Although luminescence dating has been successfully applied to many kinds of sediments from various environmental settings, dating the quartz and feldspar grains from volcanic provinces has proved challenging. One of the main reasons for this difficulty is that quartz from volcanic regions commonly emits a dim OSL signal, or no signal at all (e.g., Berger & Huntley, 1994; Fattahi & Stokes, 2003; Westaway & Roberts, 2006). The luminescence signals of feldspars are usually brighter than those of quartz from volcanic regions;

however, a high anomalous fading rate is usually observed for the blue luminescence from volcanic feldspars (Wintle, 1973; Tsukamoto & Duller, 2008; Tsukamoto et al., 2011).

Recent progress on understanding anomalous fading for feldspar provides the possibility of isolating a non-fading component in IRSL for feldspars, using either a post-IR IRSL (pIRIR) approach (Thomsen et al., 2008) or a multiple-elevated-temperature (MET) pIRIR procedure (Li & Li, 2011). These pIRIR procedures have been widely tested and applied to sediment samples from different regions in the world (see Li et al., 2014, for a comprehensive review of the progress, potential and remaining problems in using these pIRIR signals for dating). Tsukamoto et al. (2014) successfully applied a pIRIR procedure to date volcaniclastic sediments (lahar deposits) from alkaline basalts in Italy. These authors found that the laboratory fading rates of IRSL from feldspars in their samples of scoria fallout and lahar deposits can be largely reduced by applying a high preheat temperature and pIRIR stimulation temperatures, suggesting that the pIRIR method may provide a potential method for dating sediments of volcanic origin.

Previous efforts to date sediments of volcanic origins from Indonesia have used red TL or ultraviolet OSL signals from quartz, and IRSL signals from potassium-rich feldspar (K-feldspar). The OSL signals are, in general, too dim for dating purposes (Morwood et al., 2004; Roberts et al., 2009). The light-sensitive component of the red TL signal is less easily bleached than the OSL or IRSL traps, is small in size and is obtained by subtraction, resulting in imprecise and potentially inflated ages (Westaway & Roberts, 2006). The IRSL signals measured previously showed exceptionally high rates of anomalous fading and a suitable correction could not be applied. It is not until recently that the newly developed pIRIR and MET-pIRIR procedures were successfully applied to date the sediments from this region, including at the open-air site of Talepu in the Walanae Depression of South Sulawesi, which registers the earliest known presence of hominins on this island (van den Bergh et al., 2016), and at the *Homo floresiensis* type-site on Flores, the limestone cave of Liang Bua (Sutikna et al., 2016).

In this study, we tested and applied different pIRIR procedures to date volcanic sanidine extracts from the sediments from an archaeological site, Leang Bulu Bettue, on Sulawesi.

2. Study site and samples

The limestone karst border plains of Maros are located on the southwestern peninsula of the island and cover an area of approximately 400 km^2. This region contains some of the oldest surviving rock art on the planet, as demonstrated by recent U/Th dating of coralloid speleothems overlying hand stencils and large animal paintings (Aubert et al., 2014). The oldest dated rock art motif (a hand stencil) yielded a minimum age of 39.9 ka (Aubert et al., 2014). Prior to the present research, the oldest excavated archaeological findings in Maros dated to 35.6–34.5 thousand calibrated radiocarbon years before present (cal. ka BP), as revealed by excavations at Leang Burung 2 rock-shelter (Glover, 1981). Some 20 km to the north, where the karst outcrops in the adjoining Pangkep district, excavations at Leang Sakapao 1 yielded *in situ* stone artefacts and shellfish remains with a maximum age of 30–20 cal. ka BP (Bulbeck et al., 2004). In 2013–2015, we conducted deep-trench excavations at a previously uninvestigated Maros site, Leang Bulu Bettue (Fig. 1a and b), yielding cultural deposits that may exceed in antiquity the oldest evidence for humans in this karst region.

The tunnel-like cave mouth at Leang Bulu Bettue is 4 m wide and the roof at the mouth measures 3 m in height, while the interior chamber is 27.3 m long, 12.6 m wide and up to 9.2 m high (Fig. 1c). The excavated area is located just inside the entrance to the cave shelter and in an adjoining rock-shelter (inside the dripline). Our trench exposed a deeply stratified and undisturbed sequence of sedimentary layers (Fig. 1d). The archaeological contents of these layers will be reported in detail in a separate study. We provide here a brief summation of the stratigraphic sequence and cultural contents as they pertain to the uppermost (i.e., youngest) deposits (Layers 1–5), relevant to the present study. The chronological samples (i.e., radiocarbon, U-series and luminescence) were taken from the west and south wall profiles. Here we show the west wall profile only (Fig. 1d), so that all the chronological samples can be shown on a single section. Excavations into a deeper series of deposits below Layer 5, and efforts to establish a chronology for this earlier part of the stratigraphic sequence, are still ongoing.

Below the topmost layer, a thin Neolithic level (Layer 1), are cemented flowstones intercalated with calcite-rich silts (Layers 2–3). This capping flowstone unit is underlain by thin silty clays (Layers 4a and 4b) that slope downwards from the rear of the cave and level out and thicken in the main shelter, where they inter-finger with localised ashy lenses (Layers 4c–e). This combined sequence is 1.5 m thick. Below this is a 50 cm-thick sandy clay (Layer 4f) that is preserved only near the eastern wall of the cave, and which is underlain by a 50 cm-thick sandy clay (Layer 5). Layers 4a–f yielded rich cultural remains, including abundant evidence for pigment processing and use. Stone artefacts and fossil fauna are present in much lower densities in Layer 5. The chronology of the upper part of the Leang Bulu Bettue section (Layers 1–5) was established using AMS ^{14}C dating of freshwater gastropod (*Tylomelania perfecta*) shells, solution multi-collector inductively coupled plasma mass spectrometry (MC-ICP-MS) U- series dating of *in situ* stalagmites, laser ablation (LA) U-series dating of faunal remains, and luminescence dating. The location and results of the chronological samples are shown in Fig. 1d.

Layer 1 has a maximum radiocarbon age (on *in situ* charcoal) of 1.7–1.6 cal. ka BP (Wk-37740). No charcoal or other plant carbon or materials suitable for ^{14}C-dating was found below Layer 1. However, several stalagmites were recovered from the upper surfaces of both Layers 4a and 4b. These speleothems were intact, still in upright position, and had formed on top of cemented pedestals of brecciated archae-

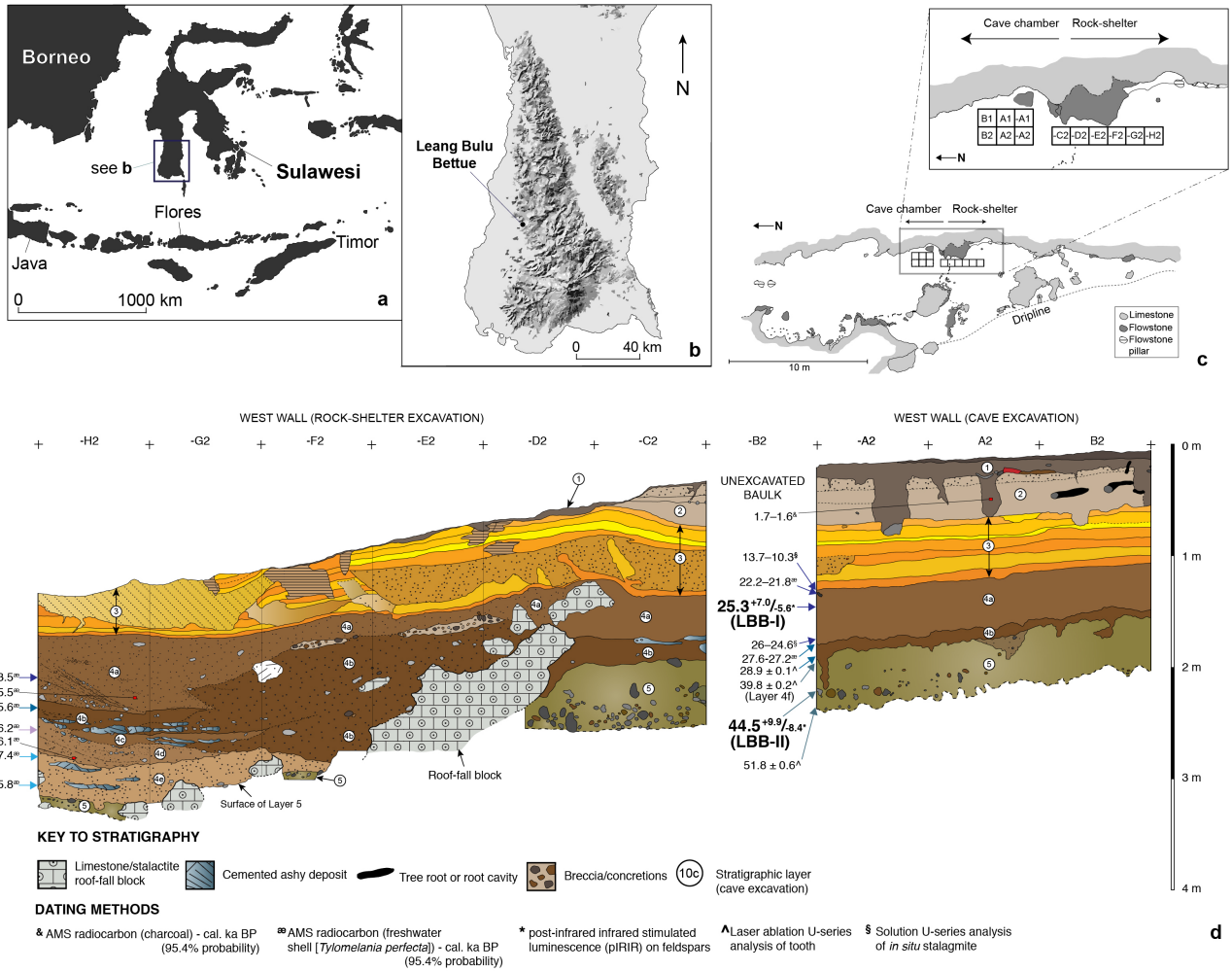

Figure 1. (a and b) Location of Leang Bulu Bettue in the Maros karsts of Sulawesi, Indonesia. (c) Plan of Leang Bulu Bettue indicating the location of the excavations. (d) Stratigraphic profile of the west walls of the excavated trenches. Sample locations and resultant age determinations for luminescence samples LBB-I and LBB-II, as well as stalagmites and (most) faunal remains, are shown projected on the west trench faces at approximate depths and according to stratigraphic layer, rather than in the original sample locations. Sample LBB-I was collected from the south wall of Square A2 and LBB-II was collected from the south wall of Square A1 (sections not shown here). The date for Layer 4f is shown in relative stratigraphic position as Layer 4f is only evident in the southeast walls of the excavated trenches (not shown here). With the exception of the calibrated radiocarbon ages, all age determinations are reported in thousands of years (ka).

ological sediment, indicating that they are *in situ* and not redeposited from other locations within the cave. Solution MC-ICP-MS U-series dating of a 30 cm high mound-like stalagmite that grew on the upper surface of Layer 4a shows that this speleothem formed between 13.7 ka to 10.3 ka ago, with the former providing a minimum age for this deposit. An 18 cm high stalagmite from the top of underlying Layer 4b was also dated using the solution MC-ICP-MS U-series technique. This stalagmite formed between 26 ka to 24.5 ka ago, allowing us to bracket the time-depth of Layer 4a to between 13.7 ka and ∼26 ka ago. A *T. perfecta* shell recovered *in situ* from close to the top of Layer 4a (131 cm depth), ∼10 cm below the cemented pedestal of archaeological detritus underlying the Layer 4a dated stalagmite, yielded an AMS ^{14}C age of 18,126 ± 51 BP (22.8–21.8 cal. ka BP at 2σ). This ^{14}C date is consistent with the associated speleothems earliest known growth stage (13.7 ± 1.8 ka), and hence we contend that it provides a reasonable estimate for the upper age of Layer 4a (i.e., ∼22.3 cal. ka BP).

Furthermore, a pig molar recovered *in situ* from Layer 4b yielded a minimum LA U-series age of 28.9 ± 0.1 ka, which is consistent with the stalagmite chronology. Layers 4b–e span ∼30–26 ka, as inferred from solution MC-ICP-MS U-series dating of the overlying stalagmite, LA U-series analysis of faunal remains, and AMS ^{14}C dating of *T. perfecta* shells. An anoa tooth from Layer 4f yielded a minimum LA U-series age of 39.8 ± 0.2 ka, suggesting this unit spans ∼40–30 ka. Similarly, LA U-series analysis of a bovid molar from the base of Layer 5 provided an in- sequence minimum age of 51.8 ± 0.6 ka.

To contribute further to the accuracy and reliability of the chronology for this site we conducted and tested the IRSL

and pIRIR procedures on two sedimentary samples taken from Layers 4a and 5, respectively, from the south wall profile. The uppermost sample LBB-I was collected from the middle of the Layer 4a, which, as already noted, is bracketed by the stalagmite and *T. perfecta* shell recovered for ^{14}C dating from the upper part of Layer 4a and the stalagmite from atop the underlying unit, Layer 4b. Sample LBB-II was collected from the middle of Layer 5. Both samples were taken by hammering 20-cm long opaque plastic tubes (5 cm in diameter) into the cleaned section face. The tubes were removed and wrapped in light-proof plastic for transport to the Luminescence Dating Laboratory at the University of Wollongong. Additional bags of sediment were collected from the tube holes and sealed in zip-lock plastic bags for laboratory measurements of sample radioactivity and field water content (see Sec. 3).

Under dim red laboratory illumination, each sample was treated using standard procedures to extract sand-sized grains of K-feldspar (Aitken, 1998). First, any carbonates and organic matter were removed using solutions of HCl acid and H_2O_2, respectively. The remaining material was then dried and mineral grains of 90–180 μm and 180–212 μm in diameter were separated by sieving. The sanidine feldspar grains were isolated from quartz and heavier minerals (using a sodium polytungstate solution of density 2.58 g/cm^3) and then etched in 10 % HF acid for 40 min to clean the grain surfaces and remove (or greatly reduce in volume) the outer α-irradiated layer of each grain. The etched sanidine feldspar grains were given a final rinse in HCl acid to remove any precipitated fluorides, and were then dried.

3. Environmental dose rate determination

Mineralogy analysis of the sediments from Leang Bulu Bettue suggests that the stratigraphic units exhibit a homogeneous pyroclastic composition dominated by calcite and sanidine feldspars (from ∼20 % to ∼80 %), and negligible quartz (only ∼1–2 %). The high percentage of sanidine feldspars in mineral composition of the sediments from Leang Bulu Bettue indicates that these feldspars are likely to be volcanic and to originate from the Camba Formation in the highlands to the east of the Maros karsts (McDonald, 1976).

The dose rate for the K-feldspars consists of 4 components: the external gamma, β- and cosmic-ray dose rates, and the internal β-dose rate. The γ-dose rate was not measured in the field, so we estimated this component from thick-source alpha counting (TSAC) measurements of U and Th and from X-ray fluorescence (XRF) measurements of K using sediments collected from the 30-cm sphere surrounding the sampling tubes, which captures the penetrating range of most gamma rays in sediments. The β-dose rate was measured directly by a Risø GM-25-5 multicounter system (Bøtter-Jensen & Mejdahl, 1988; Jacobs & Roberts, 2015) using the sediment samples recovered from each tube. The minor contribution from cosmic rays was estimated from the burial depth and water content of each sample, the thickness of cave roof overhead (∼80 m), the zenith angle dependence of cosmic rays, and the latitude, longitude and altitude of Leang Bulu Bettue (Prescott & Hutton, 1994). These external components of the total dose rate were adjusted for sample water content, using the measured (field) water content of each sample (which ranged from 29 % to 35 %) and also an assumed water content of 30 % for all samples; in all cases, we used a value of ± 5 % as the standard error of the mean to capture the likely range of time-averaged values for the entire period of sample burial. For the internal dose rate calculation, a K concentration of 10 ± 2 % (following Smedley et al., 2012) is assumed based on the theoretical K concentration of 10.69 % for sanidine, and a Rb concentration of 400 ± 100 ppm was assumed (Huntley & Hancock, 2001). The dosimetry data for all samples are summarised in Table 1.

4. Equivalent dose determination

4.1. Luminescence equipment

IRSL measurements were made using an automated Risø TL-DA-20 reader equipped with IR diodes (870 Δ 40 nm) for stimulation (Bøtter-Jensen et al., 2003). These delivered a total IR power of ∼135 mW/cm^2 to the sample position. Irradiations were carried out using a $^{90}Sr/^{90}Y$ β-source mounted on the reader. IRSL signals were detected using an Electron Tubes Ltd 9235B photomultiplier tube fitted with Schott BG-39 and Corning 7-59 filters to transmit only wavelengths of 320–480 nm. Aliquots were prepared by mounting the etched K-feldspar grains as a monolayer of ∼5 mm diameter in the centre of a 9.8 mm diameter stainless steel disc, using Silkospray silicone oil as an adhesive; this resulted in each aliquot containing several hundred grains. It is noted that we have measured 1,000 individual grains from sample LBB-I using an IR laser (830 Δ 10 nm, 400 W/cm^2) (Bøtter-Jensen et al., 2003), and we found that less than 1 % of the grains gave detectable IRSL signals. So we consider that the IRSL signal from single aliquot containing a few hundred grains may likely to be emitted from only one or a few grains.

4.2. Single-aliquot pIRIR procedures

In this study, the samples were firstly analysed using the multiple elevated temperature (MET) pIRIR procedure of Li & Li (2011). This procedure utilises the IRSL signals measured by progressively increasing the stimulation temperature from 50 °C to 250 °C in steps of 50 °C. Li & Li (2011) reported that the sensitivity-corrected MET-pIRIR signals obtained at elevated temperatures (> 200 °C) exhibited negligible rates of anomalous fading, thereby avoiding the need for any fading correction. This procedure was successfully applied to date the sediments from the Talepu site on the same island (van den Bergh et al., 2016). However, our initial measurements of K-feldspar extracts from the Leang Bulu Bettue samples revealed that they emitted very weak IRSL signals, which prevented D_e determination using the MET-pIRIR procedure. Fig. 2a shows typical MET-pIRIR signals

Table 1. Burial depths, grain sizes, water contents, dosimetry data, D_e and ages for the sanidine feldspar samples from Leang Bulu Bettue.

Sample	**Depth** (cm)	**Grain size** (μm)	**Water content** (%)	$\dot{D}_{\gamma}$ (Gy/ka)	$\dot{D}_{\beta_{external}}$ (Gy/ka)	$\dot{D}_{\beta_{internal}}$ (Gy/ka)	$\dot{D}_{cosmic}$ (Gy/ka)	$\dot{D}_{total}$ (Gy/ka)	**Isochron** D_e[(a)] (Gy)		**Age**[(b)] (ka)	
									$IRSL_{100}$ & $pIRIR_{290}$	$pIRIR_{290}$	$IRSL_{100}$ & $pIRIR_{290}$	$pIRIR_{290}$
LBB-I (Layer 4a)	160	180–212	30 ± 5 (29)	2.258 ± 0.106	2.642±0.205	0.67 ± 0.15	0.08 ± 0.01	5.65 ± 0.28	87^{+12}_{-10}	153^{+39}_{-31}	$13.7^{+2.2}_{-1.9}$	$25.3^{+7.0}_{-5.6}$
LBB-II (Layer 5)	197	90–180	30 ± 5 (30)	2.178 ± 0.097	2.222 ± 0.170	0.48 ± 0.13	0.07 ± 0.01	4.95 ± 0.23	200^{+26}_{-23}	230^{+48}_{-40}	$38.4^{+5.6}_{-5.0}$	$44.5^{+9.9}_{-8.4}$

[(a)]The isochron D_e were obtained from the intercepts of the pink lines ($pIRIR_{290}$) and blue lines ($IRSL_{100}$ and $pIRIR_{290}$) on the y-axis in Fig. 8. The error terms are 1 σ.

[(b)]The final ages are those obtained from $pIRIR_{290}$ signals. All the ages were calculated by subtracting the residual doses from corresponding D_e values.

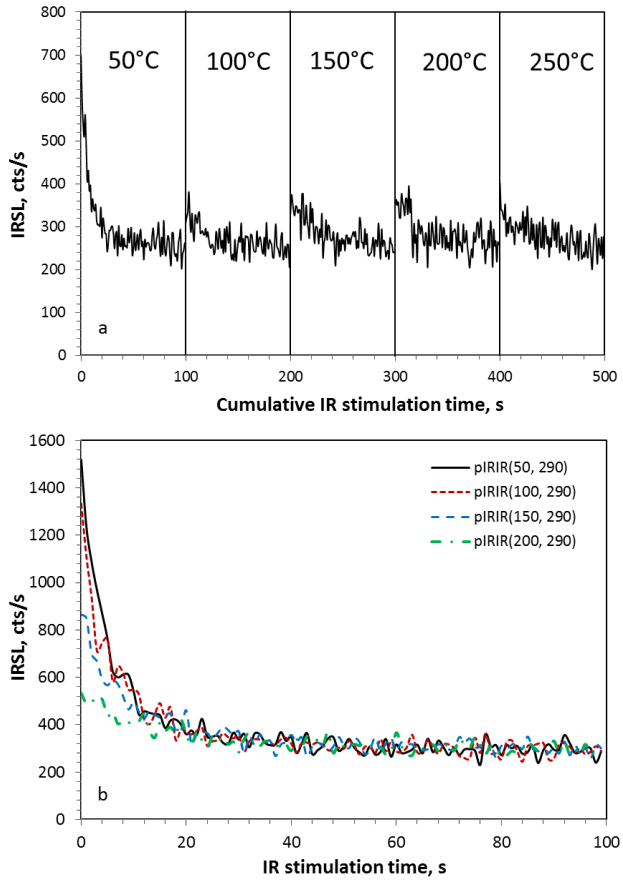

Figure 2. (a) Typical natural MET-pIRIR curves for K-feldspar grains from sample LBB-II, measured at different stimulation temperature (as indicated above each curve). (b) Typical $pIRIR_{290}$ signals from the same sample obtained after IR bleach at different temperatures from 50 °C to 200 °C.

observed for sample LBB-II at different stimulation temperatures. Even at a stimulation temperature of 250 °C, the decay of MET-pIRIR signal is negligible, presumably due to the cumulative loss of signal following multiple stimulations at lower temperature. As a result, we could not date the Leang Bulu Bettue samples using the MET-pIRIR procedure.

To measure the dim feldspar grains at Leang Bulu Bettue, we tested the two-step $pIRIR_{290}$ procedure of Thiel et al. (2011) (Table 2), in which an IR bleach is given at a low temperature (e.g., ∼50 °C) before the IRSL signal is measured at a high temperature (290 °C), because the $pIRIR_{290}$ signal is usually more intense than the 250 °C MET-pIRIR signal. It was suggested that a small rate of fading of the $pIRIR_{290}$ signal has a negligible effect on the calculated age of samples with D_e values less than ∼500 Gy (Li & Li, 2012), so it is hoped that the $pIRIR_{290}$ procedure should produce reliable estimates of D_e for the Leang Bulu Bettue samples. Fig. 2b shows the typical $pIRIR_{290}$ signals obtained after IR bleach at different temperatures from 50 °C to 200 °C. Here we will use the term $pIRIR_{(T1,T2)}$ to refer to the temperatures used in the different two-step pIRIR procedures - where T1 is the first IR stimulation temperature and the T2 is the post-IR

Table 2. The two-step $pIRIR_{290}$ procedure

Step	Treatment	Observed
1	Give regenerative dose[(a)]	
2	Preheat at 320 °C for 60 s	
3	IRSL measurement at T1 for 200 s	$L_{x(T1)}$
4	IRSL measurement at T2 (290 °C) for 200 s	$L_{x(290C)}$
5	Give test dose	
6	Preheat at 300 °C for 60 s	
7	IRSL measurement at T1 for 200 s	$T_{x(T1)}$
8	IRSL measurement at T2 (290 °C) for 200 s	$T_{x(290C)}$
9	IR bleach at 325 °C for 100 s	
10	Return to step 1	

[(a)]For the natural sample, the given dose = 0 Gy and the observed signals are L_n and T_n. The procedure is repeated for several regenerative doses, including a zero dose and a repeat dose.

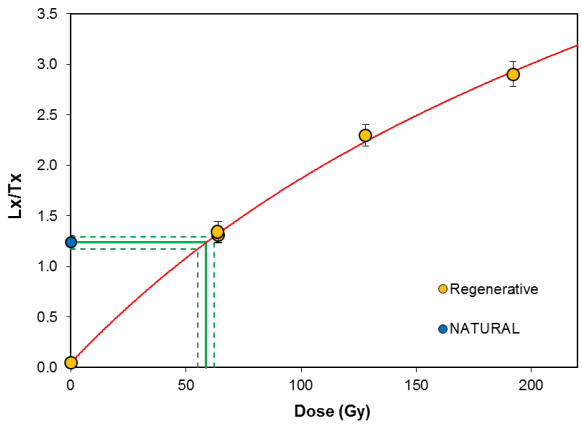

Figure 3. (a) Typical dose response curve for a single aliquot of LBB-II, showing the sensitivity-corrected $pIRIR_{(50,290)}$ natural and regenerative dose signals. The curve has been fitted to the regenerative dose data using a saturating exponential function.

stimulation temperature (T2 is fixed at 290 °C in our study). As seen from Fig. 2b, much brighter pIRIR signals were observed at a stimulation temperature of 290 °C, especially for $pIRIR_{(50,290)}$ and $pIRIR_{(100,290)}$ signals, which allowed the D_e to be determined with a reasonable precision. We also noted that the signal intensity decreases significantly as the first IR stimulation temperature is above 100 °C (e.g., 150 °C and 200 °C). We, therefore, focus on the $pIRIR_{(50,290)}$ and $pIRIR_{(100,290)}$ signals only in the following study.

4.3. D_e estimation using the $pIRIR_{(50,290)}$ procedure

The D_e values of the Leang Bulu Bettue samples were firstly measured using the $pIRIR_{(50,290)}$ procedure with a preheat at 320 °C for 60 s following either natural or regenerative doses and test doses. Typical dose response curve for one of the aliquots from LBB-II is shown in Fig. 3. The extent of recuperation and the recycling ratio are obtained routinely during construction of the dose response curve for D_e estimation (Fig. 3). It is found that, for most of the aliquots, the recycling ratios are consistent with unity and recuperation values are generally less than 10 % (i.e., the signal intensity measured after a zero dose relative to the natural intensity). Those aliquots that had recycling ratio outside the range 0.90–1.10 were discarded for D_e determination.

The $pIRIR_{(50,290)}$ D_e values obtained for LBB-I are shown in Fig. 4. A wide range of D_e values is observed for all of the samples; that is, the over-dispersion (OD) values of the distributions range from 50 % to 80 %. Based on the pattern of the D_e distribution, it may suggest that the sample might suffer from incomplete bleaching prior to burial. In this case, the minimum age model (MAM) could be applied to estimate the D_e values (Galbraith et al., 1999; Galbraith & Roberts, 2012). To test whether or not incomplete bleaching is the reason for the broad D_e distribution, the MAM was applied to estimate age for sample LBB-I, and compared with the U-series ages for the stalagmites and the ^{14}C age for the *T. perfecta* shell taken from the same layer (Fig. 1). Assuming an OD value of 20 % for well bleached samples, the MAM yield a D_e value of 10.7 ± 3.6 Gy, corresponding to an age of 2.0 ± 0.7 ka. This age, however, significantly underestimates the U-series time range of the stalagmite from atop Layer 4a, which is estimated to have formed between 13.7 ka and ∼26 ka ago. Similarly, a MAM age of 2.8 ± 1.3 ka was obtained for the sample LBB-II. This sample was taken from layer 5, which is below the two dated stalagmites, so it is expected to be older than ∼30–40 ka. Hence, the MAM ages of both LBB-II and I clearly underestimate the true ages by a substantial margin. We noted that assuming a different OD value ranging from 10 % to 30 % does not change the results significantly. We therefore conclude that the MAM should not be applied to estimate D_e values for our samples and incomplete bleaching is not the main reason for the broad D_e distributions observed.

An alternative explanation for the wide spread of D_e values is that there was a significant mixture of grains of different ages. This is, however, also unlikely because the stratigraphy of the section is horizontal and shows no evidence of post-depositional disturbance (Fig. 1d). Multiplying the dose rate of LBB-I by the ^{14}C age (∼22 ka) for the *T. perfecta* shell from the upper part of Layer 4a and the U-series age (∼26 ka) of the stalagmite from the upper surfaces of Layer 4b allows us to estimate the expected D_e value for the sample LBB-I, which lies between ∼125 Gy and ∼148 Gy. If we compare the $pIRIR_{(50,290)}$ D_e values from individual aliquots of sample LBB-I with the expected D_e (see Fig. 4), it is observed that most of the $pIRIR_{(50,290)}$ D_e values are underestimated. Since one of the most possible reasons for underestimation in IRSL dating of feldspar is anomalous fading, the underestimation in $pIRIR_{(50,290)}$ D_e values suggest that the $pIRIR_{(50,290)}$ may also suffer from anomalous fading. To confirm this, 8 aliquots from sample LBB-II were measured for an anomalous fading test. A single-aliquot measurement procedure similar to those described by Auclair et al. (2003), but based on the $pIRIR_{(50,290)}$ procedure, was applied. The fading rates (*g*-values) were calculated for the $pIRIR_{(50,290)}$ signal and normalised to the time of prompt measurement

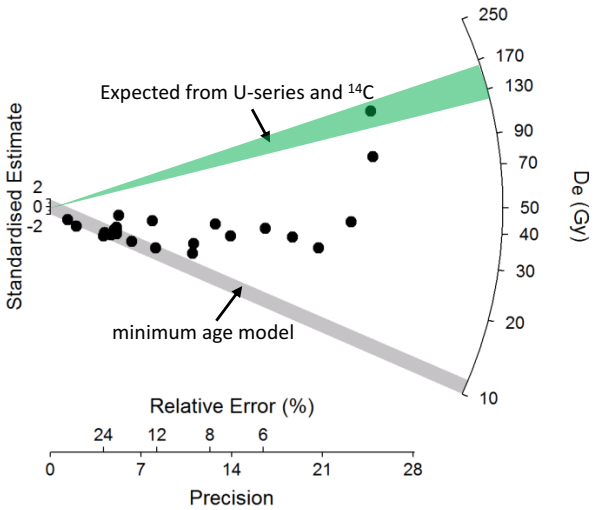

Figure 4. Radial plots showing the D_e distributions of the $pIRIR_{(50,290)}$ signals for the sample LBB-I. The green shaded area shows the expected D_e range based on multiplying the dose rate of LBB-I by the U-series ages of the two stalagmites from the upper surfaces of both Layers 4a and 4b. The grey shaded area shows the D_e value calculated using the minimum age model (MAM).

of the IRSL signal (t_c = 970 s). The *g*-values obtained are shown in Fig. 5a for individual aliquots and are summarised in the histogram in Fig. 5b. As demonstrated in Fig. 5a and Fig. 5b, a large range of *g*-values is observed, from a negligible value consistent with zero to a much higher value of ∼12 %/decade, although the *g*-values are generally associated with large uncertainties due to the low signal intensity of our samples. The results indicate that the anomalous fading rates of the $pIRIR_{(50,290)}$ signals are highly variable among different aliquots or grains, which could result in the large variation in the D_e values shown in Fig. 4. We conclude, therefore, that an IR bleaching at 50 °C for 200 s is not sufficient to remove the signals associated with the easy-to-fade traps for our samples. It should be noted that the 50 °C IRSL signals are too dim to allow for reliable estimation of fading rates.

4.4. D_e estimation using the $pIRIR_{(100,290)}$ procedure

It has been demonstrated that the stimulation temperature in the prior IR stimulation may play an important role in reducing anomalous fading for the pIRIR signals (Li & Li, 2011). Li & Li (2012) suggested that an IR stimulation at 50 °C may be insufficient to remove all of the easy-to-fade signals, but increasing the prior-IR stimulation temperature may be helpful to remove the fading component more effectively. Li & Li (2012) suggested that an IR stimulation at 200 °C is sufficient to remove all the easy-to-fade signals for their Chinese loess samples. Unfortunately, however, the dim IRSL signal from Leang Bulu Bettue prevents the application of a high IR stimulation up to 200 °C. As demonstrated in Fig. 2b, a prior IR stimulation at 150 °C or above results in a significant drops in the intensity of the subsequent $pIRIR_{290}$

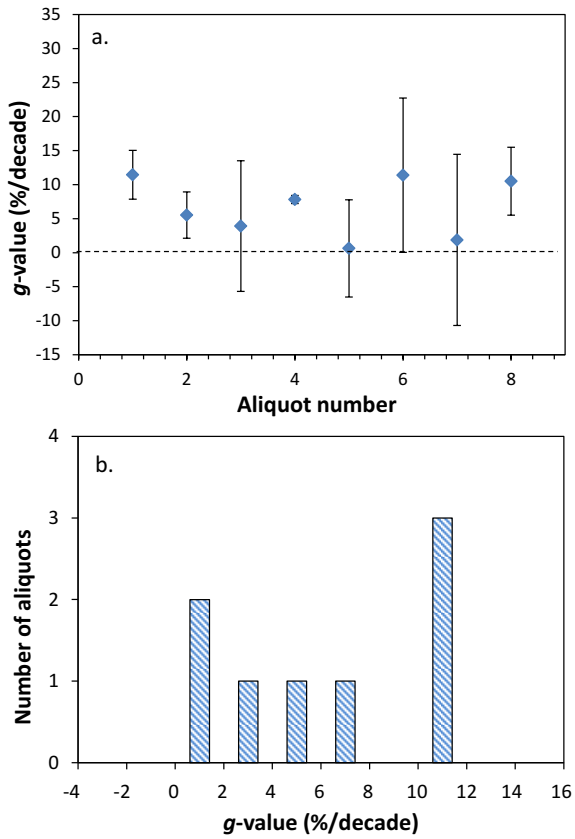

Figure 5. (a) The *g*-values of $pIRIR_{(50,290)}$ signals for 8 aliquots from sample LBB-II. (b) Histogram of the *g*-values shown in (a).

signals. Instead, a prior IR stimulation at 100 °C does not reduce the subsequent $pIRIR_{290}$ signal considerably. We therefore adopted the $pIRIR_{(100,290)}$ procedure to test whether it is possible to reduce the anomalous fading rate in the $pIRIR_{290}$ signal for our samples more effectively.

We first chose the sample LBB-I to test the $pIRIR_{(100,290)}$ procedure, as the age of this sample is well confined by the U-series stalagmite and ^{14}C ages from the same layer (Layer 4a). A total of 40 aliquots were measured and their corresponding $pIRIR_{(100,290)}$ D_e values were summarised in radial plot (Fig. 6a) and histogram (Fig. 6b), respectively. For comparison, the $pIRIR_{(50,290)}$ D_e values from 23 aliquots from the same sample were also shown in the same figures. As seen, it appears that increasing the prior IR stimulation from 50 °C to 100 °C do help to increase the D_e values in the $pIRIR_{290}$ signals. For example, the $pIRIR_{(100,290)}$ D_e values are systematically higher than the $pIRIR_{(50,290)}$ D_e values (Fig. 6b). However, a large scatter is still observed in the $pIRIR_{(100,290)}$ D_e values and most of them are still significantly underestimated when compared to the expected value based on the U-series and ^{14}C ages (Fig. 6a). The results indicate that the $pIRIR_{(100,290)}$ procedure may be able to reduce the fading component more effectively than the $pIRIR_{(50,290)}$ procedure, but it still cannot completely remove the fading component.

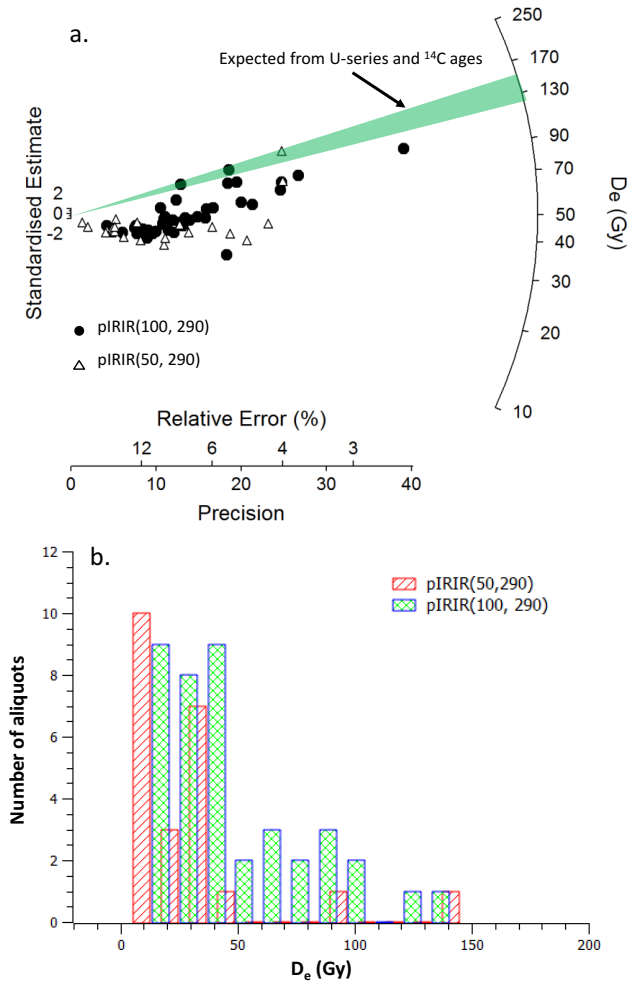

Figure 6. (a) Radial plot showing the D_e distributions of the $pIRIR_{(50,290)}$ and $pIRIR_{(100,290)}$ signals for LBB-I. The green shaded area in (a) shows the expected D_e range based on multiplying the dose rate of LBB-I by the U-series ages of the two stalagmites from the upper surfaces of both Layers 4a and 4b. (b) The same data sets in (a) displayed as histograms.

4.5. The relationship between D_e and g-value

One straightforward way to deal with anomalous fading is to correct for this phenomenon based on laboratory fading test or g-values (e.g., Huntley & Hancock, 2001; Kars et al., 2008). However, the fading correction procedures are model dependent, and may produce unreliable results. Huntley & Hancock (2001) pointed out that their fading correction procedure may result in overcorrection for a high fading rate (e.g., above ∼6 %/decade) and it should only be applied to samples with natural doses lying in the linear region of the corresponding dose response curves.

Therefore, the fading correction procedure of Huntley & Lamothe (2001) should not be applied to the $pIRIR_{290}$ results for our samples because high anomalous fading rates were observed. Although the correction method proposed by Kars et al. (2008) seems not to suffer from this problem, the large uncertainties in the g-values measured for our samples, due to the low signal intensity, result in significantly large or infinite uncertainties in the fading-corrected ages. An alternative method to deal with anomalous fading is to isolate a non-fading signal for dating, based on either pIRIR or MET-pIRIR procedures (e.g., Thomsen et al., 2008; Li & Li, 2011). We have demonstrated that a simple $pIRIR_{(50,290)}$ or $pIRIR_{(100,290)}$ procedure cannot isolate a non-fading signal for our samples, and it is impractical to apply a MET-pIRIR procedure or a $pIRIR_{(200,290)}$ procedure to overcome this problem due to the low sensitivity of the samples studied (Fig. 2). Based on the results from LBB-I, we note that the highest D_e values, for both of the $pIRIR_{(50,290)}$ and $pIRIR_{(100,290)}$ signals, are consistent with that expected from U-series dating (Fig. 4 and Fig. 6a). This indicates that the aliquots or grains associated with the highest D_e values may have negligible fading. To test this, the same aliquots used for $pIRIR_{(100,290)}$ D_e estimation were subsequently measured for anomalous fading test based on the $pIRIR_{(100,290)}$ procedure. Fig. 7 shows the histograms of the g-values obtained from the 100 °C IRSL and $pIRIR_{290}$ signals for individual aliquots measured for each of the samples. It shows that systematically higher anomalous fading rates, ranging from ∼5 %/decade to 22 %/decade, were obtained for the 100 °C IRSL signal. The g-values obtained from the $pIRIR_{290}$ signal are, however, dominated in the range of ∼ 0–12 %/decade.

The results shown in Fig. 7 suggest that, although the 100 °C IR stimulation is able to reduce the anomalous fading rate by more than the IR stimulation at 50 °C, a wide range of g-values was still observed for the $pIRIR_{290}$ signal from different aliquots. The results indicate that different aliquots may underestimate the true D_e or age in different extents. It is, therefore, expected that there should be a negative correlation between the D_e values and corresponding g-values for different aliquots from the same sample; that is, those aliquots having lower g-values should have higher D_e values, and vice versa.

To test this, the g-values obtained from the 100 °C IRSL and $pIRIR_{290}$ signals were plotted against their corresponding D_e values for individual aliquots in Fig. 8a and Fig. 8b for each of the samples, respectively. A clear negative correlation between the g-values and D_e was observed for all the samples (note the log scale on the y-axis for the D_e values; see discussions below), confirming that it is the variable fading rates among different aliquots that results in the large variation and different extents of underestimation in the D_e values.

The negative relationship between D_e value and fading rate for individual grains has been reported in previous studies (e.g., Lamothe & Auclair, 1999; Lamothe et al., 2012). Based on this observation, Lamothe & Auclair (1999) proposed an isochron method (so-called *fadia*) to deal with samples that have a large variation in fading rates. In their study, the authors plotted the additive-dose signal intensities measured immediately after irradiation against those measured after set periods of time for a series of grains, and obtained a linear relationship between them. The data sets were then

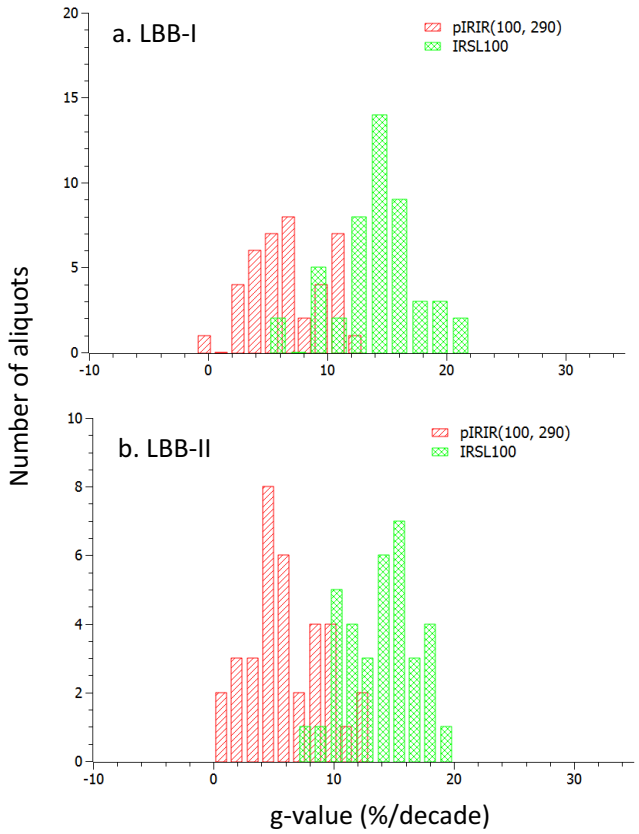

Figure 7. Histograms showing the g-values obtained from the 100 °C IRSL and $pIRIR_{290}$ signals for individual aliquots measured for each of the samples.

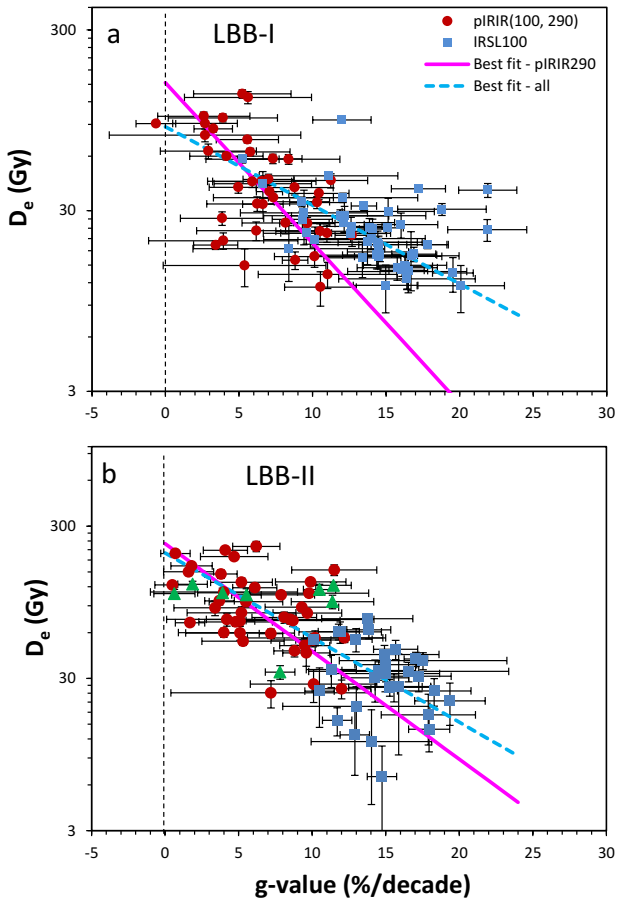

Figure 8. The D_e values obtained from the $IRSL_{100}$ and $pIRIR_{(100,290)}$ signals plotted against their corresponding g-values for individual aliquots for each of the samples, respectively. The results obtained from the $pIRIR_{(50,290)}$ signals are also shown for samples LBB-II (green triangles in b). The pink lines in the figures show the best fitting lines for the $pIRIR_{(100,290)}$ data only. The dashed blue lines show the best fitting lines for both the $IRSL_{100}$ and $pIRIR_{(100,290)}$ signals.

extrapolated to a 1 : 1 line, which represents zero fading, to correct for their additive-dose growth curves. Using a similar concept, Lamothe et al. (2012) extrapolated the trend between D_e values and g-values to a fading rate of zero, which yielded a result consistent with the expected age of their sample. For the LBB samples, we found that the relationship between the logarithm of D_e and g-value appears to broadly follow a linear relationship (Fig. 8), suggesting that an isochron method could be used to estimate D_e values at zero g-value by extrapolation onto the y-axis. In order to confirm that such a linear relationship is physically plausible, we calculated theoretical isochrons using the model described in Kars et al. (2008); Li & Li (2008). In this model, the natural and laboratory growth curves can be established for different anomalous fading rates, which allow one to calculate the apparent D_e values at different fading rates.

Fig. 9a shows the isochron lines for a series of natural doses (from 100 Gy to 1,000 Gy). It can be seen that the logarithm of the apparent D_e values have a good linear relationship with the g-values up to 12 %/decade, especially for the natural doses between 100 Gy and 600 Gy. For the natural doses larger than 600 Gy, there is a breakup of the linearity at low g-value range (e.g., 0–3 %/decade). In order to test whether one can use an isochron method to estimate the natural dose, the data series in Fig. 9a in the g-value range of 0–12 %/decade and 0–21 %/decade were linearly fitted, respectively. The isochron D_e were estimated from the intercepts of best fitting lines on the y-axis, and these are compared with the natural doses in Fig. 9b. It is shown that, for natural doses smaller than 300 Gy, fitting the data in the g-value range of 0–12 %/decade yields better results that are consistent with the natural doses within 2 %. For the natural doses from 300 Gy to 700 Gy, however, better results are produced by fitting the data from the g-value range of 0–21 %/decade (i.e., the isochron D_e are consistent with the natural doses within 3 %). For the natural dose larger than 700 Gy, the isochron D_e start to yield considerable underestimation by more than 5 %, which is expected due to the breakup of the linearity at low g-value range (Fig. 9a).

Based on this observation, we have applied linear regression onto the experimental data in Fig. 8 to estimate the D_e values corresponding to zero g-value (i.e., non-fading). We

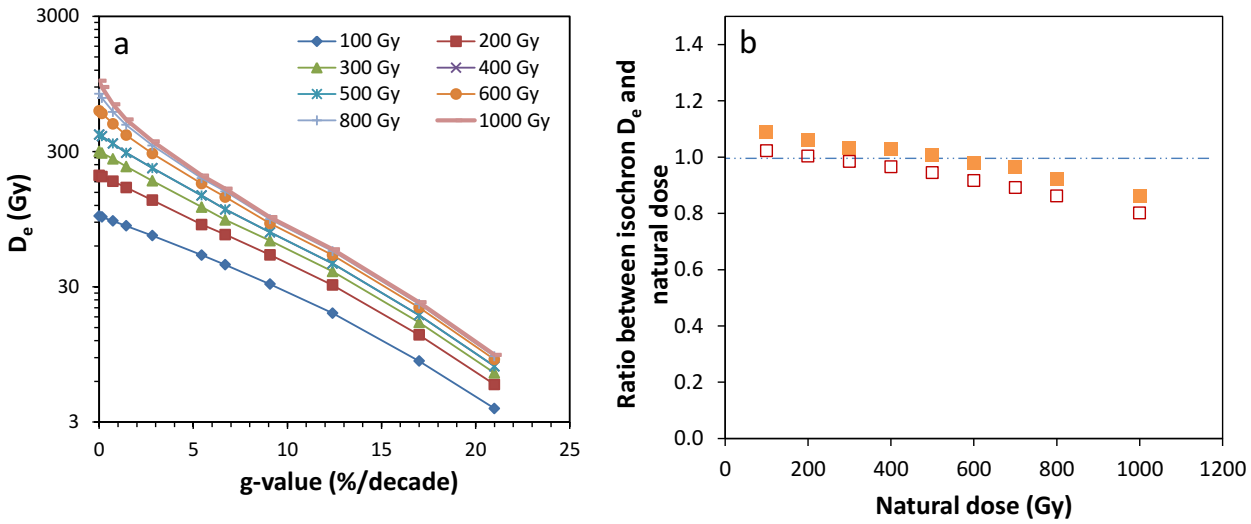

Figure 9. (a) Theoretical isochrons (D_e as a function of g-values) for different natural doses from 100 Gy to 1,000 Gy, obtained using the model described in Kars et al. (2008) and Li & Li (2008). The parameters used to produce the results are as follows: frequency factor $s = 3 \times 10^{15}\, s^{-1}$, characteristic saturation dose $D_0 = 400$ Gy, environmental dose rate= 5 Gy/ka and laboratory dose rate = 0.08 Gy/s. The D_0 and dose rates are similar to those for our samples. (b) The ratio between the isochron De and natural doses. The isochron D_e were estimated from the intercepts of linear regression using the data series of (a). The filled squares were obtained by fitting the data in the g-value range of 0–21 %/decade, while the open squares were obtained by fitting only the data in the range of 0–12 %/decade.

have used the Model 3 linear regression algorithm implemented in Isoplot 3.75 (Ludwig, 2012), which combines the errors associated with both the x- and y-values. For the sample LBB-I, this yields a D_e estimate of 153^{+39}_{-31} Gy by fitting the data set of $pIRIR_{(100,290)}$ only (pink line). This corresponds to an age of $25.1^{+6.9}_{-5.5}$ ka after correction for the residual dose (see below). If both the data sets of $pIRIR_{(100,290)}$ and $IRSL_{100}$ signals are fitted (dashed blue line), a D_e estimate of $87.4^{+12}_{-10.3}$ Gy is obtained, which corresponds to an age of $13.6^{+2.2}_{-1.9}$ ka after correction for the residual dose. Although both ages are consistent with the U- series ages of ~13.7–26 ka obtained from the stalagmites bracketing the sample, the age ($13.6^{+2.2}_{-1.9}$ ka) obtained by fitting both data sets is younger than the ^{14}C age for the *T. perfecta* shell taken above the sample. Hence, we consider the age obtained based on the data of $pIRIR_{(100,290)}$ as being more reliable. Two suppositions can explain the underestimation of the age obtained by including the data of $IRSL_{100}$ for fitting: (1) most of the g-values of the $IRSL_{100}$ signal are larger than 10 %/decade, which lies on the sublinear part of the isochron lines (Fig. 9a); (2) the D_e values of the $IRSL_{100}$ signals are very low (most of them are less than 30 Gy), so it is possible that the effect of thermal transfer or residual dose may have a significant contribution to the apparent D_e estimates. As a result, the D_e values of the $IRSL_{100}$ signal from some aliquots with high g-values may be higher than those expected according to their fading rate. For this reason, we consider that the age produced by fitting both the data sets of $pIRIR_{(100,290)}$ and $IRSL_{100}$ signals should be viewed as a minimum age estimate.

We adopted the same method to determine the D_e for the other sample LBB-II (see Fig. 8b), and the isochron of $pIRIR_{(100,290)}$ signal (pink lines in Fig. 8) yields a D_e value of 230^{+48}_{-40} Gy. The isochron obtained by fitting both $IRSL_{100}$ and $pIRIR_{(100,290)}$ signals give D_e value of 200^{+26}_{-23} Gy for the same sample. The luminescence ages from Leang Bulu Bettue, together with 1σ uncertainties obtained for all our samples, are summarised in Table 1. Our results suggest that the sampled sediments in Layers 4a and 5 were deposited $25.1^{+6.9}_{-5.5}$ ka and $44.1^{+9.8}_{-8.2}$ ka ago, respectively. These ages are in correct stratigraphic order, and the age estimate for LBB-I is consistent with the high-precision U-series ages obtained for the stalagmites bracketing Layer 4a and the ^{14}C age for the *T. perfecta* shell taken from the upper part of this layer (Fig. 1). Moreover, as noted above, LA U-series analysis of a bovid molar from the base of Layer 5 provided an in-sequence minimum age of 51.8 ± 0.6 ka, which is stratigraphically consistent with our depositional age of $44.5^{+9.8}_{-8.2}$ ka (1σ) for the sample LBB-II.

This coherent sequence of ages for the upper part of the stratigraphic sequence, and the consistency with the independent age control at this site, further supports the reliability of the isochron method proposed in this study and our contention that the feldspar grains were bleached to a low level (corresponding to a residual dose of ~10 Gy, see the next section) prior to deposition.

4.6. Residual signal and dose recovery test for the $pIRIR_{(100,290)}$ procedure

It has been shown previously that the elevated temperature pIRIR traps are not fully bleached even after prolonged sunlight exposure, and this can result in significant residual

doses at the time of sediment deposition (e.g., Thomsen et al., 2008; Li & Li, 2011; Li et al., 2013). To estimate the extent of any residual dose, we exposed 4 natural aliquots of each sample to a solar simulator for ∼4 h and the remnant doses were measured using the $pIRIR_{(100,290)}$ procedure in Table 2. The residual doses obtained are 11.5 ± 1.1 Gy and 12.6 ± 1.8 Gy for LBB-I and -II, respectively. These values were then subtracted from the D_e estimate to determine final ages for our samples.

The performance of the $pIRIR_{(100,290)}$ procedure was tested using a dose recovery test (Galbraith et al., 1999). Similar to the residual dose measurement, 4 natural aliquots from LBB-II were bleached in a solar simulator for 4 h and then given a β-dose of 80 Gy. These aliquots were then measured using the $pIRIR_{(100,290)}$ procedure. A recovered dose of 93 ± 5 Gy was obtained, corresponding to a recovery ratio of 1.00 ± 0.07, after correction for residual dose, indicating that the experimental conditions used here are able to recover the given dose accurately.

5. Discussion

Our study on the sanidines from the Leang Bulu Bettue sediments demonstrates the presence of high anomalous fading rates in the IRSL signals from sanidines, which resulted in a severe age underestimation for these samples. Our results further support the results of previous studies that high temperature and disordered volcanic feldspars, such as sanidines, generally have higher fading rates than orthoclases and microclines (Aitken, 1985; Visocekas et al., 1994, 1998; Huntley & Lian, 2006). We also show that the high anomalous fading rates cannot be overcome using a $pIRIR_{290}$ procedure for most of the aliquots measured, although the $pIRIR_{290}$ signals exhibit a much less pronounced fading rate compared to the prior IRSL signals measured at lower temperature (50 °C or 100 °C). Furthermore, it appears that different grains or aliquots from our samples have considerably different fading rates in their IRSL and pIRIR signals, which results in a large among-aliquot variation in their corresponding D_e values (Fig. 4, 5, 6, 7). Such a wide spread in D_e values could easily lead to a false impression that these samples have been insufficiently bleached or contain a mixture of grains with different ages, which may result in erroneous age estimation if a minimum age model was adopted (Fig. 4). We suggest, therefore, that it is important to conduct a detailed anomalous fading test when using pIRIR procedure, especially for dating volcanic feldspars. We proposed a method to deal with the problem associated with variable fading rate encountered for dating the sanidine feldspars from the archaeological site Leang Bulu Bettue, based on the relationship between the D_e values and g-values (Fig. 8). Our method is, in principle, similar to the method of Lamothe & Auclair (1999) and Lamothe et al. (2012) proposed to deal with samples that have a large variation in fading rates. In their studies, the authors extrapolated the linear relationship between D_e and g-value. In our study, in contrast, we extrapolated of the relationship between the $log(D_e)$ values and g-values, based on numerical simulation using the physical model of Huntley & Lian (2006). Our results suggest that reliable D_e estimate can be obtained by extrapolation of the relationship between the $log(D_e)$ values and g-values to zero fading (i.e., g-value = 0 %/decade). The pIRIR ages obtained for our samples are consistent with the empirical results from other independent dating techniques from the same site, confirming the validity of the isochron method.

6. Conclusions

The volcanic sanidines from two Late Pleistocene archaeological layers at Leang Bulu Bettue on the Indonesian island of Sulawesi have a highly variable anomalous fading rate in their IRSL signal for different grains and aliquots. The dim IRSL signal intensity prevents the application of a MET-pIRIR procedure, and a low temperature IR stimulation (at 50 °C or 100 °C) used in a $pIRIR_{290}$ procedure cannot completely remove the anomalous fading for the subsequent $pIRIR_{290}$ signals. Reliable D_e estimation can be achieved by extrapolation of the relationship between D_e and g-values for the same sample, which provides a useful way to date the sediments containing volcanic feldspars of similar luminescence characteristics.

Acknowledgments

The dating work was supported by an Australian Research Council Future Fellowship to B.L. (FT140100384), an Australian Research Council Australian Laureate Fellowship to R.G.R. (FL130100116), and a postgraduate scholarship from the China Scholarship Council and the University of Wollongong to Y.G. (201206010053). The Leang Bulu Bettue excavations were funded by an Australian Research Council (ARC) DECRA fellowship (DE130101560) to A.B., with additional support provided by the Wenner Gren Foundation (Post-Ph.D. grant), University of Wollongong, and Griffith University. The Indonesian fieldwork was authorised by RISTEK and the Pusat Penelitian Arkeologi Nasional (ARKENAS). For facilitating this research, we thank ARKENAS director I.M. Geria, and the former directors of Makassars Balai Pelestarian Cagar Budaya and Balai Arkeologi, M. Said and G.M. Sudarmika, respectively. We also acknowledge the support of Y. Jafari and T. Lachlan in the Luminescence Dating Laboratory at the University of Wollongong. Fieldworkers included: B. Burhan, A.M. Saiful, L. Siagian, Suryatman, R. Sardi, A. Jusdi, Abdullah, A. P. Mubarak, Hasliana, Hasrianti, D. Susanti, R. Salempang, H. Arsyad, Muhtar, Sungkar, R. Ali, L. Lantik, Asri, H. Lahab, O. Amrullah, Idrus, M. Husain, Busran, A. Agus and D.P. McGahan.

References

Aitken, Martin J. *Thermoluminescence dating*. Studies in archaeological science. Academic Press, 1985.

Aitken, Martin J. *An Introduction to Optical Dating*. Oxford University Press, 1998.

Aubert, M, Brumm, A, Ramli, M, Sutikna, T, Saptomo, E W, Hakim, B, Morwood, M J, van den Bergh, G D, Kinsley, L, and Dosseto, A. *Pleistocene cave art from Sulawesi, Indonesia*. Nature, 514(7521): 223–227, 2014.

Auclair, Marie, Lamothe, Michel, and Huot, S. *Measurement of anomalous fading for feldpsar IRSL using SAR*. Radiation Measurements, 37(4-5): 487–492, 2003.

Berger, G W and Huntley, D J. *Tests for optically stimulated luminescence from tephar glass*. Quaternary Science Reviews, 13 (5-7): 509–511, 1994.

Bøtter-Jensen, L and Mejdahl, V. *Assessment of beta dose-rate using a GM multicounter system* . Nuclear Tracks and Radiation Measurements, 14: 187–191, 1988.

Bøtter-Jensen, L, Andersen, C E, Duller, Geoff A T, and Murray, Andrew S. *Developments in radiation, stimulation and obersservation facilities in luminescence measurements*. Radiation Measurements, 37: 535–541, 2003.

Bulbeck, D, Sumantri, I, and Hiscock, P. *Leang Sakapao 1, a second dated Pleistocene site from South Sulawesi, Indonesia*. In Keates, Susan G and Pasveer, Juliette M (eds.), *Quaternary Research in Indonesia*, pp. 111–128. 2004.

Fattahi, Morteza and Stokes, Stephen. *Dating volcanic and related sediments by luminescence methods: a review*. Earth-Science Reviews, 62: 229–264, 2003.

Galbraith, Rex F and Roberts, Richard G. *Statistical aspects of equivalent dose and error calculation and display in OSL dating: An overview and some recommendations*. Quaternary Geochronology, 11: 1–27, 2012.

Galbraith, Rex F, Roberts, Richard G, Laslett, G M, Yoshida, H, and Olley, J M. *Optical dating of single and multiple grains of Quartz from Jinmium Rock Shelter, Northern Australia: Part I, Experimental design and statistical models*. Archaeometry, 41 (2): 339–364, 1999.

Glover, I C. *Leang Burung 2: an Upper Palaeolithic rock shelter in south Sulawesi, Indonesia*. Modern Quaternary Reasearch in Southeast Asia, pp. 1–38, 1981.

Huntley, D J and Hancock, R G V. *The Rb contents of the K-feldspar grains being measured in optical dating*. Ancient TL, 19(2): 43–46, 2001.

Huntley, D J and Lamothe, Michel. *Ubiquity of anomalous fading in K-feldspars and the measurement and correction for it in optical dating*. Canadian Journal of Earth Sciences, 38: 1093–1106, 2001.

Huntley, D J and Lian, Olav B. *Some observations on tunnelling of trapped electrons in feldspars and their implications for optical dating*. Quaternary Science Reviews, 25(19-20): 2503–2512, 2006.

Jacobs, Zenobia and Roberts, Richard G. *An improved single grain OSL chronology for the sedimentary deposits from Diepkloof Rockshelter, Western Cape, South Africa*. Journal of Archaeological Science, 63(C): 175–192, 2015.

Kars, R H, Wallinga, J, and Cohen, K M. *A new approach towards anomalous fading correction for feldspar IRSL dating — tests on samples in field saturation*. Radiation Measurements, 43: 786–790, 2008.

Lamothe, Michel and Auclair, Marie. *A solution to anomalous fading and age shortfalls in optical dating of feldspar minerals*. Earth and Planetary Science Letters, 171: 319–323, 1999.

Lamothe, Michel, Barré, Magali, Huot, Sébastien, and Ouimet, Stéphanie. *Natural luminescence and anomalous fading in K-feldspar*. Radiation Measurements VL -, 47(9): 682–687, 2012.

Li, Bo and Li, Sheng-Hua. *Investigations of the dose-dependent anomalous fading rate of feldspar from sediments*. Journal of Physics D: Applied Physics, 41(22): 225502, 2008.

Li, Bo and Li, Sheng-Hua. *Luminescence dating of K-feldspar from sediments: A protocol without anomalous fading correction*. Quaternary Geochronology, 6(5): 468–479, 2011.

Li, Bo and Li, Sheng-Hua. *A reply to the comments by Thomsen et al. on "Luminescence dating of K-feldspar from sediments: A protocol without anomalous fading correction"*. Quaternary Geochronology, 8(C): 49–51, 2012.

Li, Bo, Roberts, Richard G, and Jacobs, Zenobia. *On the dose dependency of the bleachable and non-bleachable components of IRSL from K-feldspar: Improved procedures for luminescence dating of Quaternary sediments*. Quaternary Geochronology, 17: 1–13, 2013.

Li, Bo, Jacobs, Zenobia, Roberts, Richard, and Li, Sheng-Hua. *Review and assessment of the potential of post-IR IRSL dating methods to circumvent the problem of anomalous fading in feldspar luminescence*. Geochronometria, 41(3): 178–201, 2014.

Ludwig, Kenneth R. *User's Manual for Isoplot 3.75*. Berkeley Geochronology Center, 3.75 edition, 2012.

McDonald, R C. *Limestone morphology in South Sulawesi, Indonesia*. Zeitschrift für Geomorhologie, Supplementbände, 26: 79–91, 1976.

Morwood, M J, Soejono, R P, Roberts, R G, Sutikna, T, Turney, C S M, Westaway, K E, Rink, W J, Zhao, J x, van den Bergh, G D, Due, Rokus Awe, Hobbs, D R, Moore, M W, Bird, M I, and Fifield, L K. *Archaeology and age of a new hominin from Flores in eastern Indonesia*. Nature, 431(7012): 1087–1091, 2004.

Prescott, J. R. and Hutton, J T. *Cosmic ray contributions to dose rates for luminescence and ESR dating: Large depths and long-term time variations*. Radiation Measurements, 23(2-3): 497–500, 1994.

Roberts, R G, Westaway, K E, Zhao, J x, Turney, C S M, Bird, M I, Rink, W J, and Fifield, L K. *Geochronology of cave deposits at Liang Bua and of adjacent river terraces in the Wae Racang valley, western Flores, Indonesia: a synthesis of age estimates for the type locality of Homo floresiensis*. Journal of Human Evolution, 57(5): 484–502, 2009.

Smedley, R K, Duller, G A T, Pearce, N J G, and Roberts, H M. *Determining the K-content of single-grains of feldspar for luminescence dating*. Radiation Measurements VL -, 47(9): 790–796, 2012.

Sutikna, Thomas, Tocheri, Matthew W, Morwood, Michael J, Saptomo, E Wahyu, Jatmiko, Awe, Rokus Due, Wasisto, Sri, Westaway, Kira E, Aubert, Maxime, Li, Bo, Zhao, Jian-xin, Storey, Michael, Alloway, Brent V, Morley, Mike W, Meijer, Hanneke J M, van den Bergh, Gerrit D, Grün, Rainer, Dosseto, Anthony, Brumm, Adam, Jungers, William L, and Roberts, Richard G. *Revised stratigraphy and chronology for Homo floresiensis at Liang Bua in Indonesia*. Nature, 532(7599): 366–369, 2016.

Thiel, Christine, Buylaert, J P, Murray, Andrew, Terhorst, Birgit, Hofer, Ingo, Tsukamoto, Sumiko, and Frechen, Manfred. *Luminescence dating of the Stratzing loess profile (Austria) - Testing the potential of an elevated temperature post-IR IRSL protocol*. Quaternary International, 234(1-2): 23–31, 2011.

Thomsen, K J, Murray, Andrew S, Jain, M, and Bøtter-Jensen, L. *Laboratory fading rates of various luminescence signals from feldspar-rich sediment extracts*. Radiation Measurements, 43(9-10): 1474–1486, 2008.

Tsukamoto, S and Duller, G A T. *Anomalous fading of various luminescence signals from terrestrial basaltic samples as Martian analogues*. Radiation Measurements, 43(2-6): 721–725, 2008.

Tsukamoto, S, Duller, G A T, Wintle, A G, and Muhs, D. *Assessing the potential for luminescence dating of basalts*. Quaternary Geochronology, 6(1): 61–70, 2011.

Tsukamoto, Sumiko, Kataoka, Kyoko, Oguchi, Takashi, Murray, Andrew S, and Komatsu, Goro. *Luminescence dating of scoria fall and lahar deposits from Somma-Vesuvius, Italy*. Quaternary Geochronology, 20(C): 39–50, 2014.

van den Bergh, Gerrit D, Li, Bo, Brumm, Adam, Grün, Rainer, Yurnaldi, Dida, Moore, Mark W, Kurniawan, Iwan, Setiawan, Ruly, Aziz, Fachroel, Roberts, Richard G, Suyono, Storey, Michael, Setiabudi, Erick, and Morwood, Michael J. *Earliest hominin occupation of Sulawesi, Indonesia*. Nature, pp. 1–19, 2016.

Visocekas, R, Spooner, N A, Zink, A, and Blanc, P. *Tunnel afterglow, fading and infrared emission in thermoluminescence of feldspars*. Radiation Measurements, 23(2-3): 377–385, 1994.

Visocekas, R, Tale, V, Zink, A, and Tale, I. *Trap Spectroscopy and Tunnelling Luminescence in Feldspars*. Radiation Measurements, 29(3-4): 427–434, 1998.

Westaway, Kira E and Roberts, Richard G. *A dual-aliquot regenerative-dose protocol (DAP) for thermoluminescence (TL) dating of quartz sediments using the light-sensitive and isothermally stimulated red emissions*. Quaternary Science Reviews, 25 (19-20): 2513–2528, 2006.

Wintle, Ann G. *Anomalous Fading of Thermoluminescence in Mineral Samples*. Nature, 245: 143–144, 1973.

Reviewer

Jim Feathers

Reviewer's comment

Michel Lamothe and colleagues introduced the idea of isochron dating to address the problem of anomalous fading in 1999 and then followed up in 2012. The paper here by Bo Li and colleagues develops this idea further and shows the strength of a too-long neglected method. The application here is to volcanic feldspars, but it would be worth pursuing other applications.